# Silicon wavelength-selective partial-drop broadcast filter bank

**Zhan Su,[1] Matteo Cherchi,[1] Erman Timurdogan,[1] Jie Sun,[1] Michele Moresco,[1] Gerald Leake,[2] Douglas Coolbaugh,[2] and Michael R. Watts[1,*]**

[1]*Research Laboratory of Electronics, Massachusetts Institute of Technology, Cambridge, Massachusetts 02139, USA*

[2]*College of Nanoscale Science and Engineering, University at Albany, Albany, New York 12203, USA*

**Corresponding author: mwatts@mit.edu*

Received June 19, 2014; revised August 8, 2014; accepted August 8, 2014;
posted August 11, 2014 (Doc. ID 214378); published September 15, 2014

We propose an approach to a wavelength-selective $1 \times N$ port optical broadcast network demonstrating the approach in a $1 \times 8$ port parallel optical drop filter bank utilizing adiabatic micro-ring tunable filters. The micro-ring filters exhibit first-order $92.7 \pm 3.7$ GHz full width at half-maximum bandwidths with a 36.2 nm free spectral range, low-drop power variation (0.11 dB), and aggregate excess loss of only 1.1 dB in all drop ports. Error-free operation at a 10 Gbit/s data rate is achieved for all eight drop ports with less than a 0.5 dB power penalty among the ports. This wavelength-selective parallel-drop approach serves as a building block for on-chip all-to-all communication networks. 

*OCIS codes:* (130.3120) Integrated optics devices; (230.5750) Resonators; (230.0250) Optoelectronics.
http://dx.doi.org/10.1364/OL.39.005459

With the scaling of chip multicore microprocessor systems, communications between the cores on chip and between the cores and memory systems off chip have become the limiting factor affecting system performance [1]. Integrated photonics provide a solution for both on- and off-chip communications, enabling massive bandwidths with low power consumption [2,3]. In on-chip computer networks, bus (or broadcast) topologies are among the most widely deployed, enabling all-to-all communications for rapid dissemination of instructions and data across a machine. Recently, it has been proposed that wavelength-selective all-to-all communications, with the transmit wavelength being tied to a particular core, offer a particularly compelling implementation on chip for all-to-all networks [4]. Using integrated photonic devices, bus topologies can be implemented by cascaded power splitters [5] connected to multiprocessors; however, with simple power dividers, all wavelengths must be dropped at all sites along the network, limiting the potential network topologies. Importantly, a limitation of pure all-to-all topologies is that the optical power requirements scale with $N^2$, where $N$ is the number of sites. As a result, for large-scale implementations, limited all-to-all topologies, where the information is shared among a select group of sites, are often more attractive. In order to implement limited all-to-all communications networks, wavelength-selective partial drops are required [see Fig. 1(a)] [6] with a select group of wavelengths. The most challenging component of the all-to-all communications network is shown in Fig. 1(b). The resonant detectors can be implemented by connecting drop ports of ring resonators to on- or off-chip detectors [inset of Fig. 1(b)] but are not essential for demonstrating the parallel-drop functionality. Thus, for the rest of this Letter, the broadcast network in Fig. 1(b) will be simplified to a parallel optical drop filter bank with off-chip detectors.

Previously, single large-radius rings with multiple drop ports have been utilized to act as a wavelength-selective power divider [7]. However, the limited free spectral range (FSR) makes that approach incompatible with dense wavelength division multiplexed communications. To overcome those limitations, small-radius ring resonators are preferred to enable large FSRs and wide optical bandwidth in the on-chip network.

In this Letter, we introduce a new wavelength-selective on-chip optical broadcast network based on integrated small-radius tunable resonant filters, which offer high tuning efficiency and large FSR [8,9] to support densely packed wavelength channels. The theory on how to design an arbitrary $N$-stage system is presented, and a $1 \times 8$ parallel optical partial-drop filter bank is demonstrated with a 3 dB bandwidth of 92.7 GHz and standard deviation across all eight ports of only 3.7 GHz. The aggregate excess loss of the parallel drop is only 1.1 dB with optical power variation of only 0.11 dB. Error-free

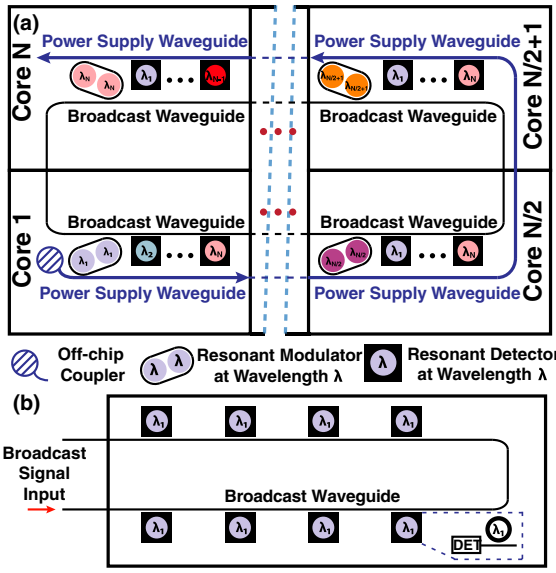


Fig. 1. (a) Example approach of wavelength-selective partial-drop filters utilized in an all-to-all communications network. (b) One × eight on-chip broadcast network demonstrated in this work. Inset, implementation of resonant detector at wavelength $\lambda_1$.

 

operation at a 10 Gbit/s data rate is demonstrated for all eight drop ports, with less than a 0.5 dB power penalty. This approach will enable future applications such as on-chip optical multi-casting and high-sensitivity transmitters and receivers in on-chip wavelength division multiplexing (WDM) networks [10].

Conventionally, optical ring-based filters utilize a symmetric configuration, where ring-to-waveguide coupling strengths are the same on both the through and drop ports. This corresponds to matched ring–waveguide separations and results in full power dropping at resonance with Lorentzian filter responses for a first-order filter. However, by adjusting the ring-to-waveguide separations to be asymmetric, partial power dropping can be implemented while maintaining a Lorentzian filter response around the resonant wavelength. By cascading partial-drop filters, wavelength-selective power dropping can be engineered to produce equal drops with identical filter responses through a careful adjustment of the coupling coefficients. To prove that identical Lorentzian filter responses can be achieved in a cascaded partial-drop system, coupled-mode theory (CMT) in the time domain [11] is utilized to model the micro-ring filters.

The schematic of an $N$-stage ring-based parallel-drop filter bank is shown in Fig. 2(a). Assuming that the internal loss of the cavity is negligible compared to the coupling strength from the waveguide, the system can be described by the following equations:

$$\frac{dA^i}{dT} = -i\omega_0 A^i - \sum_{l=1}^{2}\left(\frac{A^i}{\tau_l^i} + \sqrt{\frac{2}{\tau_l^i}}S_{l+}^i\right), \tag{1}$$

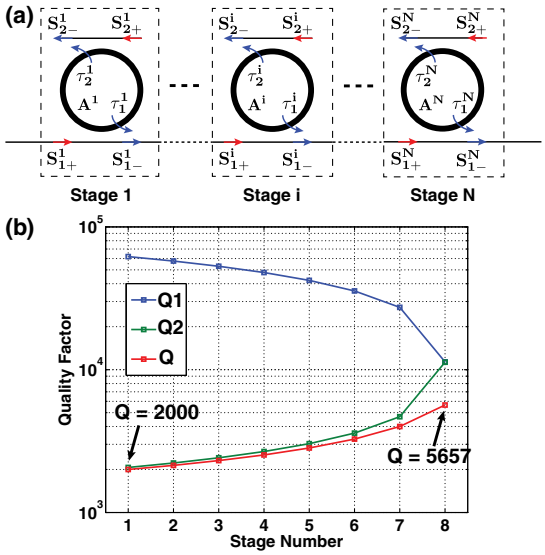


Fig. 2. (a) Schematic of an $N$-stage ring-based cascaded partial-drop filter bank. Each ring supports a circulating mode with energy amplitude $A$, incident wave amplitude $S_{1+}$, transmitted wave amplitude $S_{1-}$, drop port output wave amplitude $S_{2-}$, and input wave amplitude $S_{2+}$. $\tau$ denotes the amplitude decay time constant of each cavity through a separate waveguide. (b) Quality factors required to maintain equal drops in an eight-stage filter bank were calculated from coupled-mode theory (CMT) and plotted.

$$S_{l-}^i = -S_{l+}^i + \sqrt{\frac{2}{\tau_l^i}}A^i, \tag{2}$$

$$S_{1-}^i = S_{1+}^{i+1}, \tag{3}$$

where $\omega_0$ is the cavity resonant frequency; $A$ is the energy amplitude of the cavity, which is normalized so that $|A|^2$ represents the total energy stored in the cavity; and $S$ is the wave amplitude, which is normalized so that $|S|^2$ represents the power. The superscript $i$ represents the $i$th stage, and the + and – denote the input and output to the cavity, respectively. The time constant, $\tau$, denotes the amplitude decay time constant of the cavity due to coupling to the bus and drop waveguide. For the single input case, $S_{2+}^i$ is zero. For an input frequency $\omega$, $dA^i/dT = -i\omega A^i$. To achieve even power splitting into $N$ drop ports, it can be derived from Eqs. (1)–(3) that the following conditions need to be satisfied:

$$\tau_1^{i+1}\cdot\tau_2^{i+1} = \tau_1^i\cdot\tau_2^i, \tag{4}$$

$$\left|\frac{1}{\tau_1^{i+1}} + \frac{1}{\tau_2^{i+1}}\right| = \left|\frac{1}{\tau_2^i} - \frac{1}{\tau_1^i}\right| \tag{5}$$

for $i = 1, \ldots N-1$. Assuming that the peak power at $\omega_0$ for each port is $1/N$ of the total input power and the total decay time constant for the first stage is $\tau \equiv 1/(1/\tau_1^1 + 1/\tau_2^1)$ and $\tau_1^1 \geq \tau_2^1$, the explicit equations for $\tau_1^i$ and $\tau_2^i$ are

$$\begin{cases} \tau_1^1 = 2\left[\sqrt{N(N-1)} + N\right]\tau \\ \tau_2^1 = \frac{\sqrt{N(N-1)}+N}{\sqrt{N(N-1)}+N-\frac{1}{2}}\tau \end{cases}, \tag{6}$$

$$\begin{cases} \tau_1^{i+1} = \frac{1}{2}\left[\tau_1^i - \tau_2^i + \sqrt{(\tau_1^i)^2 + (\tau_2^i)^2 - 6\tau_1^i\tau_2^i}\right] \\ \tau_2^{i+1} = \frac{1}{2}\left[\tau_1^i - \tau_2^i - \sqrt{(\tau_1^i)^2 + (\tau_2^i)^2 - 6\tau_1^i\tau_2^i}\right] \end{cases} \tag{7}$$

for $i = 1, \ldots N-1$. Under these conditions, all the drop ports have the same Lorentzian frequency response:

$$\left|\frac{S_{2-}^i}{S_{1+}^i}\right|^2 = \frac{4/\tau_1^1\tau_2^1}{(\omega-\omega_0)^2 + \left(\frac{1}{\tau}\right)^2}, \tag{8}$$

with peak value $1/N$ and a filter response bandwidth that depends only on the chosen $\tau$ value. With a quality factor ($Q$-factor) $Q = \omega_0\tau/2$, assuming eight stages of the system and the $Q$-factor of the first stage to be 2000, the $Q$-factors for each stage are shown in Fig. 2(b). We point out that the $1/N$ equipartition condition requires that the $i$th stage drops a fraction $1/(N-i+1)$ of the optical power still left in the bus waveguide. In order to ensure the same bandwidth at each stage, the $Q$-factors of the resonators must vary. This theory can be easily extended to cases where the intrinsic loss of the filter is not negligible by including the $\tau_r$ term in Eq. (1) to represent the decay constant of energy due to the intrinsic loss of the cavity.

Following the theory discussed previously, we designed a $1 \times 8$ port parallel-drop filter bank. A schematic of the proposed device is shown in Fig. 3(a). Each of the rings has the same resonant wavelength and shares the same bus waveguide. The dependence of $\tau$ as a function of the ring-to-waveguide separation is calculated using finite-difference time-domain (FDTD) simulations. In order to compensate for (1) variations in the thickness of the silicon layer across the wafer, (2) variations in the width of the waveguide due to fluctuations in the photolithographic process [12], and (3) coupling-induced frequency shifts [13], an integrated heater is incorporated into the device utilizing an adiabatic structure [8]. The tunable adiabatic micro-ring resonator is shown in the inset of Fig. 3(a) with contacts created from doped silicon tethers.

The proposed structure was fabricated on a 300 mm silicon on insulator (SOI) wafer with a 220 nm silicon layer thickness using 193 nm optical immersion lithography. A scanning electron micrograph (SEM) of the fabricated device after dry etching to remove the top $SiO_2$ cladding is shown in Fig. 3(b). Integrated heaters are introduced by p-type doping at a concentration of $1 \times 10^{18}$ $cm^{-3}$ in the adiabatic ring waveguide, and contacts are connected to the heaters by small tethers of silicon with $p+$ doping at a concentration of $1 \times 10^{20}$ $cm^{-3}$ [inset of Fig. 3(a)]. This way, each ring in this system is independently thermally tunable. The fabricated adiabatic ring is 6 μm in diameter [inset of Fig. 3(b)], ensuring a large FSR for WDM applications.

A transverse electric (TE) polarized tunable laser was coupled into the fabricated device using a single-mode fiber (SMF), and the transmission spectra of the through port and eight drop ports were measured. Although all the ring sizes and drop port responses were designed to be identical, the resonant frequencies with no voltage applied differed from one another due to layer thickness and lithographic variations [12], as well as differing coupling-induced frequency shifts [13] for each drop port. The drop port responses reveal a resonance variation of 33.5 GHz and power difference of more than 5 dB in average wavelength of 1553.6 nm [shown in Fig. 4(a)]. The power differences mainly come from resonant wavelength variations. Wavelengths that are not filtered by previous stages tend to exhibit high power when they are filtered by the current stage. By using thermal tuning, the wavelength variation was removed. The tuning powers for each drop port are shown in Fig. 4(b). The corresponding spectra after thermal tuning are shown in Figs. 4(c) and 4(d), revealing a resonance variation as low as 1.7 GHz and a power variation of less than 0.11 dB, which are low enough to ensure equal power distributions among all drop ports. The 3 dB bandwidth variation was extracted to be 3.7 GHz with an average value of 92.7 GHz—wide and uniform enough to handle high-speed data-rate transmission for all drop ports. Moreover, the filter bank exhibits a wide, uncorrupted FSR of 36.2 nm [inset of Fig. 4(c)], enabling a large number of communication wavelength channels. Although eight rings and heaters are utilized in this device, the total loss of this parallel drop is only 1.1 dB—no worse than that for a single fully coupled filter, a result that makes sense given that, in aggregate, the coupling of the eight-way drop equates to the coupling of a single fully coupled ring.

This parallel-drop filter bank allows high-speed data to be transmitted to all eight drop ports with equal power distribution. A diagram of the experimental setup used to characterize the filter bank performance is depicted in Fig. 5(a). A continuous-wave tunable laser source was first coupled into a SMF. The light was then transmitted through a commercial lithium niobate ($LiNbO_3$) modulator with polarization controllers (PCs) before and after the modulator to align the polarization to the TE waveguide mode. In this work, the data were coded with non-return-to-zero (NRZ) on–off keying (OOK) using a pulse pattern generator (PPG) with a $2^{31} - 1$ pseudo-random bit sequence (PRBS). The modulated light was then coupled onto the silicon chip. By thermally tuning the rings, all the resonant frequencies were aligned to the same wavelength. For the input, the light of the tunable laser was spectrally aligned to the resonant wavelength to drop the signal to each drop port. Off chip, the modulated optical signal was then passed through an erbium-doped

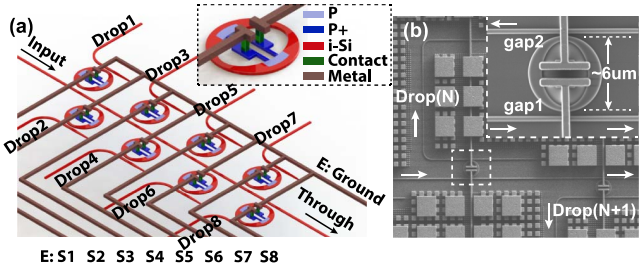


Fig. 3. (a) Schematic of the optical parallel-drop filter bank. All the micro-rings shown in the figure have the same resonant frequency with different couplings to the bus and drop waveguides. Inset, schematic of the tunable adiabatic micro-ring filter. (b) Scanning electron micrograph (SEM) of the fabricated device. Inset: a close-up view of the fabricated tunable adiabatic micro-ring filter.

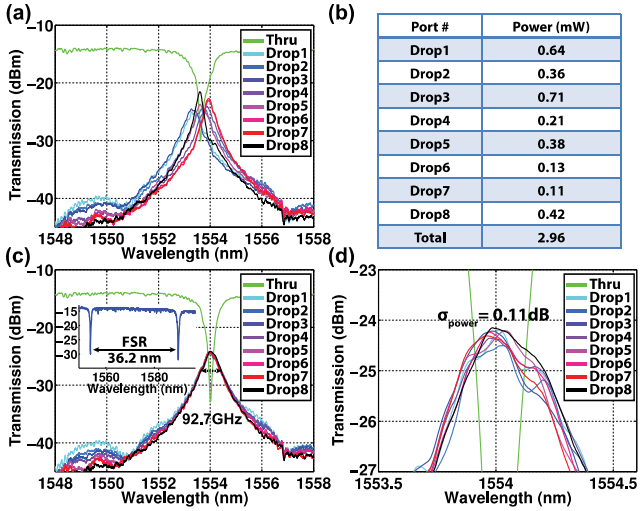


| Port # | Power (mW) |
|---|---|
| Drop1 | 0.64 |
| Drop2 | 0.36 |
| Drop3 | 0.71 |
| Drop4 | 0.21 |
| Drop5 | 0.38 |
| Drop6 | 0.13 |
| Drop7 | 0.11 |
| Drop8 | 0.42 |
| Total | 2.96 |

Fig. 4. (a) Transmission spectra of the parallel-drop filter bank before tuning. (b) Tuning power for each drop port. (c) Transmission spectra of the parallel-drop filter bank after thermal tuning. Inset: spectral response of the device showing an uncorrupted 36.2 nm free spectral range (FSR). (d) Close-up view of the transmission spectra of the parallel-drop filter bank after thermal tuning showing a power variation of 0.11 dB with 2.96 mW total tuning power.

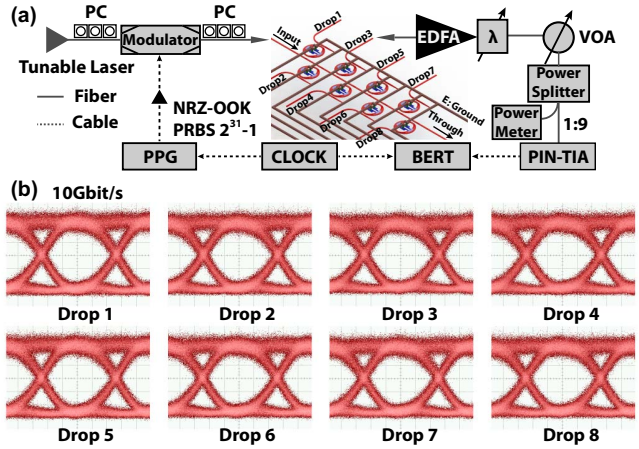


Fig. 5. (a) Experimental setup diagram for characterizing the data transmission performance. (b) Eye diagrams for Drop Ports 1–8 with 10 Gbit/s data generated from an external commercial $LiNbO_3$ modulator with input laser wavelength at 1554 nm.

fiber amplifier (EDFA), a tunable grating filter ($\lambda$) with 1 nm 3 dB bandwidth, and a variable optical attenuator (VOA). A 1:9 power splitter was used after VOA to direct 10% of the power to a power meter for monitoring while transmitting the rest of the power (~90%) to a high-speed (10 Gbit/s) PIN photodiode and transimpedance amplifier (PIN–TIA) receiver. The signal was evaluated using a bit error rate (BER) tester (BERT). Both the PPG and the BERT were synchronized to the same clock.

Figure 5(b) shows the obtained eye diagrams for all drop ports with a 10 Gbit/s data rate. The resulting diagrams are equally open. We then took the BER curves and measured the power penalty for each port using a 10 Gbit/s data rate to quantify the differences between each transmission (shown in Fig. 6). For each BER curve, we also verify error-free operation, achieving BERs below $10^{-12}$. The BER curves validate our initial observations about power uniformity across channels, showing less than a 0.5 dB power penalty difference among the channels. Although the device demonstrated has slow roll-off with first-order filter responses, limiting the channel spacing, with the help of high-order filter designs

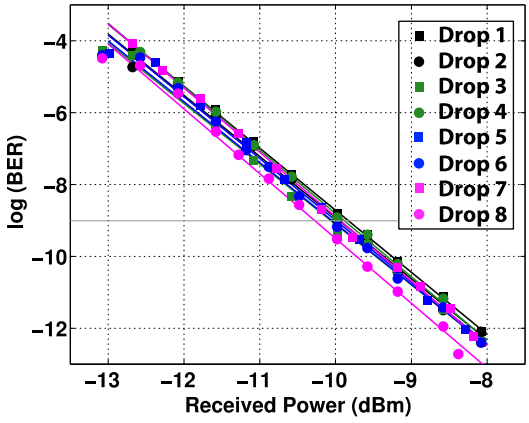


Fig. 6. Experimentally measured bit error rate (BER) curves for the partial-drop broadcast system for each drop port with 10 Gbit/s data rates generated from an external commercial $LiNbO_3$ modulator.

[14], the same technique developed can be readily applied to narrower bandwidth parallel-drop filter banks for dense wavelength division multiplexed (DWDM) applications.

In conclusion, we proposed a theoretical framework for a $1 \times N$ port ring-based parallel optical partial-drop filter bank and demonstrated the approach in a $1 \times 8$ wavelength-selective parallel filter bank based on partial-drop tunable adiabatic micro-ring filters. The micro-ring filters demonstrate low power variation (0.11 dB) among all the outputs, and a small excess loss of 1.1 dB in aggregate and error-free operation for 10 Gbit/s data rates is achieved for all eight drop ports, with less than a 0.5 dB power penalty difference among these ports. The wavelength selectivity and large FSR (36.2 nm) enabled by small-radius rings offer a promising solution to WDM optical broadcasts and high-sensitivity transmitters and receivers.

This work was supported by the Defense Advanced Research Projects Agency (DARPA) Microsystems Technology Office's (MTO) E-PHI, Grant No. HR0011-12-2-0007, and the Assistant Secretary of Defense for Research & Engineering under Air Force Contract No. FA8721-05-C-0002. Opinions, interpretations, conclusions and recommendations are those of the author and are not necessarily endorsed by the United States Government.

## References

1. R. Kumar, V. Zyuban, and D. M. Tullsen, in *Proceedings of the 32nd International Symposium on Computer Architecture* (IEEE, 2005), pp. 408–419.
2. A. Shacham, K. Bergman, and L. P. Carloni, IEEE Trans. Comput. **57**, 1246 (2008).
3. E. Timurdogan, C. M. Sorace-Agaskar, J. Sun, E. S. Hosseini, A. Biberman, and M. R. Watts, Nat. Commun. **5**, 4008 (2014).
4. N. Kirman, M. Kirman, R. Dokania, J. F. Martinez, A. B. Apsel, M. A. Watkins, and D. H. Albonesi, in *Proceedings of the 39th Annual IEEE/ACM International Symposium on Microarchitecture* (IEEE, 2006), pp. 492–503.
5. Q. Li, S. Rumley, M. Glick, J. Chan, H. Wang, K. Bergman, and R. Dutt, J. Opt. Commun. Netw. **5**, 945 (2013).
6. L. G. Kazovsky, W.-T. Shaw, D. Gutierrez, N. Cheng, and S.-W. Wong, J. Lightwave Technol. **25**, 3428 (2007).
7. D. Spencer, D. Dai, Y. Tang, M. Heck, and J. Bowers, IEEE Photon. Technol. Lett. **25**, 36 (2013).
8. M. R. Watts, W. A. Zortman, D. C. Trotter, G. N. Nielson, D. L. Luck, and R. W. Young, in *Conference on Lasers and Electro-Optics* (Optical Society of America, 2009), paper CPDB10.
9. M. R. Watts, Opt. Lett. **35**, 3231 (2010).
10. D. O. Caplan, J. J. Carney, and S. Constantine, in *Conference on Lasers and Electro-Optics* (Optical Society of America, 2011), paper PDPB12.
11. J. D. Joannopoulos, S. G. Johnson, J. N. Winn, and R. D. Meade, *Photonic Crystals: Molding the Flow of Light*, 2nd ed. (Princeton University, 2008).
12. Z. Su, E. S. Hosseini, E. Timurdogan, J. Sun, G. Leake, D. D. Coolbaugh, and M. R. Watts, in *Optical Fiber Communication Conference* (Optical Society of America, 2014), paper Th2A.55.
13. M. A. Popović, C. Manolatou, and M. R. Watts, Opt. Express **14**, 1208 (2006).
14. B. E. Little, S. T. Chu, H. A. Haus, J. Foresi, and J.-P. Laine, J. Lightwave Technol. **15**, 998 (1997).